

# Nano3YSZ electrophoretic deposition from acetylacetone + ethanol solvent on the surface of AZ91 magnesium alloy

Sahand Behrangi, Hossein Aghajani ✉

Department of Materials Engineering, University of Tabriz, Tabriz P.O.Box: 5166616471, Iran

✉ E-mail: h\_aghajani@tabrizu.ac.ir

Published in Micro & Nano Letters; Received on 18th September 2017; Revised on 20th December 2017; Accepted on 15th January 2018

In the present work, the conditions for electrophoretic deposition of yttria-stabilised zirconia (YSZ) nanopowder have been investigated. For this purpose, the mixture of acetyl acetone and ethanol with different mixing ratios was used as solvent with iodine as a dispersant. To achieve a smooth, homogeneous and crack-free coatings, the following parameters were chosen to be optimised: the mixing ratio of acetyl acetone and ethanol, voltage and duration of deposition. The obtained coatings were observed by scanning electron microscope and optical microscope. The weight of deposits was also measured in different deposition conditions to observe the effects of above-mentioned parameters on the weight and consequently the quality of green coatings. All in all, the suspensions which composed of 50 vol% acetylacetone + 50 vol% ethanol led to more uniformity and fewer cracks/pores in deposits. The other parameters were optimised as follows: deposition voltage of 40 V and deposition time of 3 min. The results of polarisation test showed an improved corrosion resistance of the magnesium alloy with the application of YSZ coating, so that the  $I_{\text{corr}}$  value decreased from 1.16 to 0.088 mA.

**1. Introduction:** Magnesium and its alloys have a high strength-to-weight ratio which made them good candidates to be used in wide variety of applications [1, 2]. However, their corrosion resistance is low which limits the wider usage of magnesium alloys [3, 4]. The most common way to overcome this problem is applying a protective coating on the surface. Therefore, several coating materials and methods have been introduced so far. Some of the methods are conversion coating [5], sol-gel [6], physical vapour deposition (VD) [7], chemical VD [8], cold spray [9], arc-glow plasma deposition [10] and electroplating [11].

Electrophoretic deposition (EPD) is another method to apply a coating on metallic substrates. EPD is defined as the movement of dispersed charged particles in a liquid medium toward the opposite electrode and formation of a deposit on it [12]. The green loose coating obtained by this process should be followed by a sintering procedure to obtain a compact and adherent deposit. Generally, EPD has some advantages such as short duration of the process, simple set-up, lower cost, the applicability on complex shapes, the possibility of controlling thickness and morphology of deposited layer with adjusting time and potential, uniformity of deposited layer and deposition of composite coatings [12–15]. In case of magnesium alloys, EPD has attracted attentions in recent years specially to improve the corrosion resistance for biomedical applications [16, 17].

The weight of deposit formed by EPD depends directly on voltage, time, suspension concentration and zeta potential value of the particles in the suspension. These mentioned parameters play an important role in the formation of a coating on a substrate by EPD method [18].

Yttria-stabilised zirconia (YSZ) is one of the most suitable materials to improve the corrosion resistance of magnesium alloys [19]. Two types of parameters, i.e. suspension parameters and deposition parameters have been studied for EPD of YSZ particles on metallic and non-metallic substrates. In case of suspension preparation and stabilisation, a wide variety of solvents and dispersants has been used so far. Ethanol [20], isopropanol [21], acetone [15], acetylacetone [18], a mixture of acetone and ethanol [22, 23] and a mixture of acetylacetone and ethanol [24, 25] are just some of the solvents that have been used. Iodine is the most useful dispersant used by several researchers to stabilise the suspension of YSZ particles in different solvents [18, 20, 21, 26]. Water has also been used as a dispersant in

some cases [20, 22]. In case of deposition parameters such as voltage, time and suspension concentration, a very wide range of values has been applied.

Several studies have been published concerning the deposition of YSZ on other substrates such as nickel (Ni) [23], Ni oxide-YSZ [20, 22, 26] and La<sub>0.85</sub>Sr<sub>0.15</sub>MnO<sub>3</sub> [18, 21, 25]. Also, some studies have been published about the deposition of other materials such as hydroxyapatite, titanium oxide, ceria etc. [27–30] on metallic alloys. However, there is no published research on EPD of YSZ on magnesium alloys. Therefore, it seems that the optimisation of the conditions for EPD of YSZ on magnesium substrate has not been exactly studied so far. Consequently, the purpose of present Letter is to determine the optimum and applicable deposition conditions to form a uniform and crack-free coating on a magnesium-based alloy.

**2. Materials and methods:** The substrate material used in this Letter was a magnesium-based alloy composed of 2.95 wt% zinc, 8.14 wt% aluminium as alloying elements. Square specimens were cut with dimensions of 12 mm × 12 mm × 3 mm. Before deposition, the samples were ground with silicon carbide papers of 100–1500 grits followed by cleaning and degreasing ultrasonically in acetone for 15 min and drying in the air.

The used nanopowder was 3 mol% YSZ (Sigma-Aldrich, USA) with a particle size of about 100 nm. Phase analysis of the YSZ powder was done using X-ray diffraction (XRD) (Bruker, Germany, Cu  $K_{\alpha}$  = 1.54 Å). The XRD pattern of this nanopowder is shown in Fig. 1.

The used solvent for preparing suspensions was a mixture of acetylacetone (99%, Merck, Germany) and ethanol (99.6%, Kimia Alcohol Zanjan, Iran) with different mixing ratios. Iodine (99.8%, Carlo Erba, France) was added as dispersant to improve the stability of suspensions.

To prepare suspensions, YSZ nanopowder was mixed with iodine and solvent. Thereafter, the mixture was stirred for 2 h on a magnetic stirrer (Alfa, Iran) followed by ultrasonication in an ultrasonic bath (Mercury, Turkey) for 1 h. To study the suspension stability, Dynamic Light Scattering (DLS) (Microtrac, Germany) was used to obtain zeta potential and mean particle size of the suspensions.

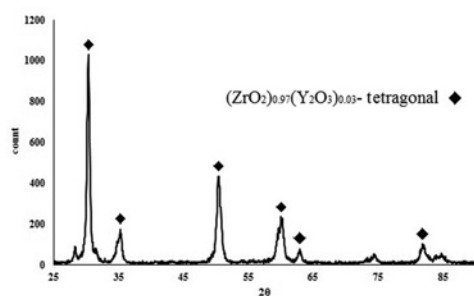


Fig. 1 XRD pattern of 3YSZ nanopowder used in this Letter

Suspension stability was studied by investigating the role of two important factors. To study the role of solvent type, acetylacetone and ethanol were mixed with proportions of 100, 75, 50, 25 and 0 vol% acetylacetone with ethanol. For each solvent, iodine concentration was varied between 0 and  $1 \text{ g l}^{-1}$  with an interval of  $0.1 \text{ g l}^{-1}$ . Therefore, the influence of solvent (mixing ratio of the two solvents) was studied as well as iodine concentration. In all of these experiments, the suspension concentration was  $10 \text{ g l}^{-1}$  and kept constant. To avoid confusion, suspensions are named 100/0, 75/25, 50/50, 25/75 and 0/100 from now on, in which the first number (before the slash) shows the volume per cent of acetylacetone and the next shows the ethanol content.

EPD was done in a 100 ml beaker with AZ91 specimens as a cathode and a  $15 \text{ mm} \times 15 \text{ mm}$  stainless steel sheet as an anode. This was due to the positive surface charge of YSZ particles in suspensions. The distance between two electrodes was adjusted to be 15 mm. Different voltages and durations were applied to study the effect of these two parameters on EPD. The voltages were 20, 40, 60 and 80 V and the durations were 2, 3, 4 and 5 min. Therefore, 16 samples were coated with each solvent. After coating, the samples were dried in a fixed volume closed vessel at room temperature for about 24 h to avoid crack formation due to rapid drying. However, the appearance of the samples shows the formation of some drying cracks. The cracks planar density (CPD) of the samples was measured by the use of Clemex image analyser software. All of these samples were weighed before and after EPD by means of digital scale (Radwag, Poland) to measure the weight of deposited YSZ. The coatings were microscopically observed with optical microscope (OM) (Lissview, China) field emission scanning electron microscope (SEM) (Tescan, Czech Republic).

The electrochemical investigation was performed using an Ivium potentiostat (Ivium Technologies, Netherland) controlled by a computer using the Ivium's software. A saturated calomel electrode and platinum were used as reference and counter electrodes, respectively, and the sample was used as working electrode, exposing  $1 \text{ cm}^2$  of the area to the 3.5% sodium chloride (NaCl) solution. The scan was conducted with a start potential of  $-1000 \text{ mV}$  until  $1000 \text{ mV}$ . From the polarisation curves, the corrosion current density ( $I_{\text{corr}}$ ) and corrosion potential ( $E_{\text{corr}}$ ) were determined using the Ivium software provided with the equipment.

### 3. Results and discussion

3.1. Suspension stability: Fig. 2 shows the zeta potential plotted versus iodine concentration. Some important points can be inferred from this diagram. Zeta potential of the particles in suspension reversely relates to the ethanol content of the solvent. As seen, an increase in the ethanol content decreases the zeta potential value. The highest values of zeta potentials belong to 100/0 suspension. This returns to the high ability of acetylacetone for production of positive ions when reacting with iodine. When iodine is used as a dispersant, some reactions between the solvent and iodine generate positive charges ( $\text{H}^+$ ) named protons. These

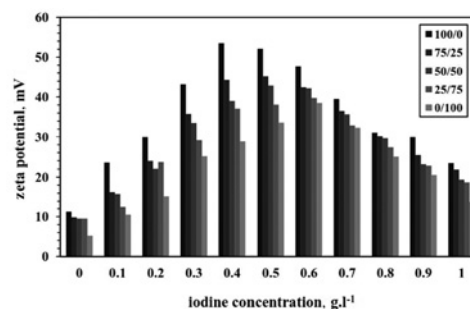


Fig. 2 Zeta potential versus iodine concentration for 100/0, 75/25, 50/50, 25/75 and 0/100 suspensions

protons are adsorbed to the particles and supply their surface charge and consequently the repulsion force between them. The reactions of ethanol and acetylacetone with iodine are as follows [20, 23]:



As seen in (1) and (2), one mole of ethanol could produce one proton; however, one mole acetylacetone could produce two protons. Therefore, with the addition of ethanol and decrement of acetylacetone, zeta potential drops.

The next point is about optimum iodine concentration and its role in suspension stability. As known, zeta potential is a criterion for stability of a suspension. According to Fig. 2, increasing iodine concentration to a specified value leads to the improvement of zeta potential. However, a descending trend is seen with further iodine increment which means the lack of suspension stability. In case of lower iodine concentrations, the zeta potential and suspension stability are low. The reason is clear because the iodine amount is not so enough to produce sufficient positive ions to completely cover the surface of all particles. When iodine is added beyond the optimum amount, zeta potential and consequently the suspension stability drops due to the compression of electrical double layer [20, 22].

The other point inferred from zeta potential diagram is the variation of optimum iodine concentration with solvent. As seen in Fig. 2, the optimum iodine concentration increases with an ethanol content of the solvent. Although this increase is not so severe and the optimum iodine concentration reaches from  $0.4 \text{ g l}^{-1}$  for 100/0 suspension to  $0.6 \text{ g l}^{-1}$  for 0/100 suspension. As seen in this figure, the highest zeta potential in the absence of iodine belongs to 100/0 suspension. This shows that with a decrease in acetylacetone content, more iodine is needed to stabilise the suspension. Therefore, the required iodine to obtain the higher stability rises.

Fig. 3 shows the plot of suspension mean particle size versus iodine concentration. A reasonable trend is also seen in this diagram which verifies the behaviour of zeta potential presented in Fig. 2. The reason for this behaviour is the gravity force. Agglomeration of particles increases the weight, gravity force and consequently suspension sedimentation. This happens mainly due to the lack of sufficient particle surface charge which leads to the domination of attractive forces on repulsive forces and agglomeration of particles. As mentioned before, the produced positive ions increase with the amount of acetylacetone in the suspension. Iodine concentration has a positive effect in inhibiting the agglomeration of particles; however, its reverse effect appears after an

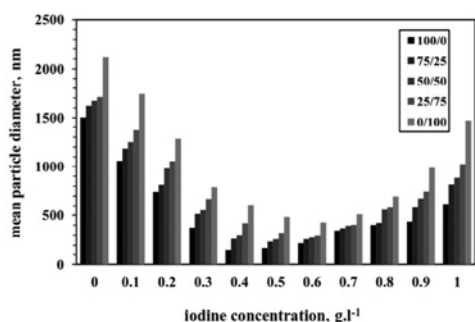


Fig. 3 Mean particle size versus iodine concentration for 100/0, 75/25, 50/50, 25/75 and 0/100 suspensions

optimum value due to the compression of the double electrical layer.

3.2. Electrophoretic deposition: In this section of the Letter, the effects of solvent and also two main process parameters which are voltage and duration of deposition were studied. As mentioned before, the applied voltages were 20, 40, 60 and 80 V and durations were 2, 3, 4 and 5 min. In case of 100/0 suspension, all of the samples had visual cracks. Fig. 4 and Table 1 show the weight gain of the substrates coated with 100/0 suspension. As can be seen, the highest deposit weight belongs to the voltage of 80 V and duration of 5 min. In lower voltages, the rate of the weight gain is ascending but with increasing voltage, a reduction in the rate of weight gain is seen especially in higher durations. In higher voltages, the earlier thickening of the deposit as an insulating layer leads to lowering the rate of the weight gain with prolonging the process time. However, at lower voltages, this is not seen due to the slighter deposition rate. The sum of the deposits' weight formed on 16 samples were 859.9 mg which is a high amount resulted in the cracking of the deposits.

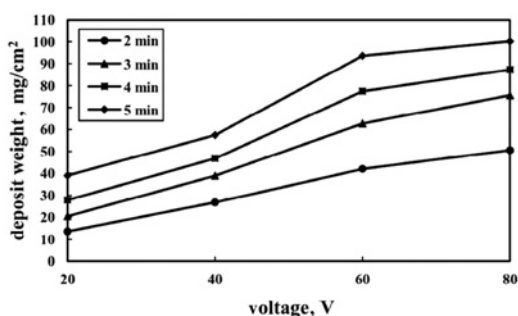


Fig. 4 Deposited weight versus applied voltage for 100/0 suspension with different durations

Table 1 Weight of coatings deposited from different suspensions

t, min	V, V															
	20				40				60				80			
	2	3	4	5	2	3	4	5	2	3	4	5	2	3	4	5
$W_{100/0}$ , mg/cm <sup>2</sup>	13.58	20.41	27.83	38.97	26.77	38.91	46.81	57.47	42.03	62.69	77.43	93.57	50.56	75.56	87.27	100.1
$W_{75/25}$ , mg/cm <sup>2</sup>	12.08	17.58	21.66	27.8	17.91	27.91	34.08	40.54	32.5	45.53	54.89	65.4	42.81	55.59	62.36	72.23
$W_{50/50}$ , mg/cm <sup>2</sup>	8.39	12.5	15.04	18.84	11.93	16.33	21.25	27.18	18.18	24.86	33.3	43.51	21.92	29.96	40.95	50.66
$W_{25/75}$ , mg/cm <sup>2</sup>	2.46	4.3	6.74	9	5.1	8.5	10.79	13.45	9.63	16.02	21.4	26.11	12.37	19.09	26.72	33.55

The high deposition rate from 100/0 suspension refers to the high zeta potential value resulted by acetylacetone medium. As mentioned before, the deposit weight is directly related to the zeta potential of the particles. Therefore, the higher the zeta potential, the higher the deposit weight. The high deposit weight is explainable with the high number of generated protons.

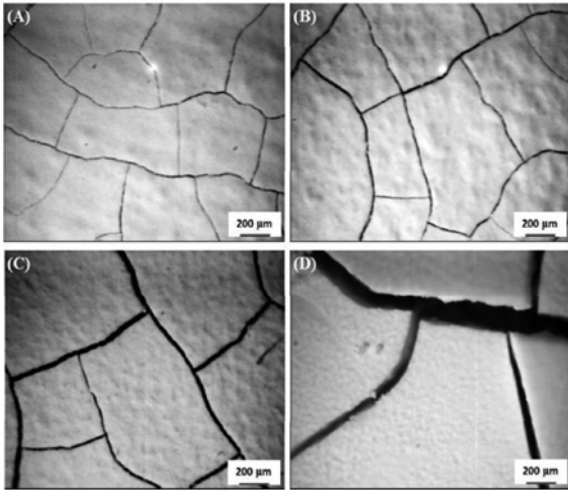
By checking the relation between deposited weight and time from data given in Table 1, it could be concluded that for nearly all samples, by increasing the duration of the coating process, the deposition rate remains constant and the weight grows linearly. Although, in some cases, a small lower rate could be observed in higher durations. It was expected that increasing the time will decrease the deposition rate. Thus, it could be concluded that the selected durations for coating process are not high enough to form a heavy thick ceramic layer that has a low electrical conductivity. In such a case, the rate of the deposition could decrease dramatically.

Fig. 5 typically shows the OM images of deposits formed on the samples. The images belong to the deposits formed with different voltages (20, 40, 60 and 80) in a constant deposition of 5 min. The effect of increasing voltage on the thickness of the deposit and consequent cracks is consistent with the results of weights presented above. This figure shows that the increasing of the voltage resulted in the formation of wider cracks which are resulted by the formation of the thicker deposit layer.

In the next step, the 75/25 suspension was used. In this case, four samples which were coated with conditions of 4/20, 5/20, 2/40 and 3 min/40 V were visually crack free. The quality of coatings was better due to the existence of ethanol in the suspension. The presence of ethanol leads to the decreasing the number of generated protons in the suspension which are adsorbed on the particles [23]. As a result, the deposit weight decreases slightly resulting in a less thick coating. Fig. 6 and Table 1 show the weight gain with voltage and duration of deposition. The reduction in deposit weights compared with 100/0 suspension is obvious, so that the sum of deposit weights for 16 samples was reduced to 630.8 mg (it was 859.9 mg for 100/0 suspension). It can be also seen that the reduction in the rate of weight gain with prolonging the deposition time is significant at higher voltages. In general, it can be concluded that the deposition conditions and qualities get better with adding 25% ethanol to the suspension.

SEM images of four visually qualified deposits obtained with above-mentioned conditions are presented in Fig. 7. The surfaces of the samples coated with the conditions of 4/20 and 5 min/20 V are not smooth and full of micropores. The surface quality of deposits formed by conditions of 2/40 and 3 min/40 V are almost similar. However, 3 min led to the formation of some cracks.

The samples with visual cracks were observed with OM. Fig. 8 shows the optical microscopic images of four typically selected samples. They were selected in a way to show the effect of deposition time (2, 3, 4 and 5 min with a constant voltage of 80 V) on the formation of cracks. Increasing the number of cracks and their depths is obvious with an increment of deposition time due to the thickening of deposit as seen in Fig. 6 and Table 1.



**Fig. 5** Optical microscopic images of samples coated from 100/0 suspension with voltages of  
 a 20 V (CPD=6%)  
 b 40 V (CPD=7.5%)  
 c 60 V (CPD=10%)  
 d 80 V (CPD=14%) for 5 min

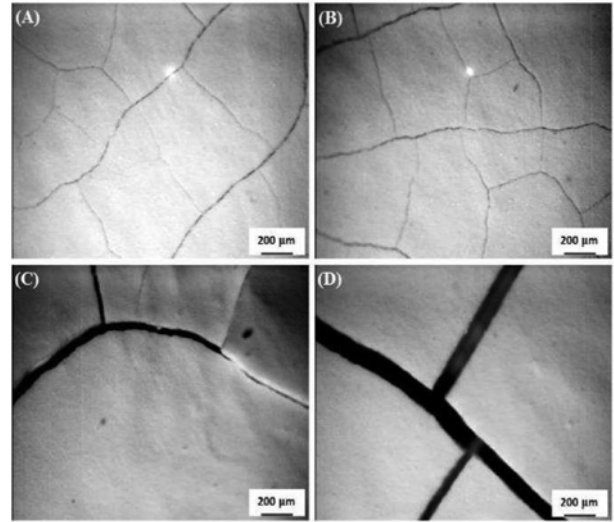


**Fig. 8** Optical microscopic images of samples coated from 75/25 suspension with voltage of 80 V and durations of  
 a 2 min (CPD=6%)  
 b 3 min (CPD=7%)  
 c 4 min (CPD=9%)  
 d 5 min (CPD=13.5%)

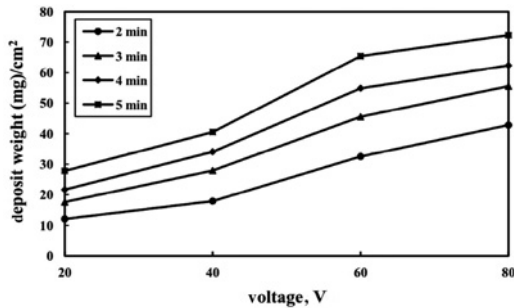


**Fig. 6** Deposited weight versus applied voltage for 75/25 suspension with different durations

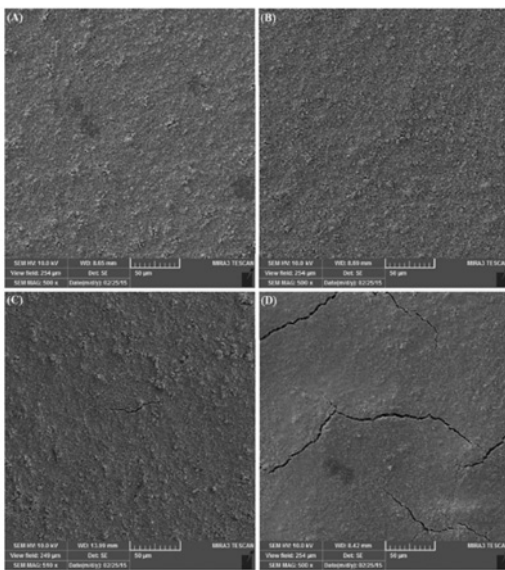


**Fig. 7** SEM images of coatings deposited from 75/25 suspension by conditions of  
 a 4 min/20 V  
 b 5 min/20 V  
 c 2 min/40 V  
 d 3 min/40 V

The 50/50 suspension was the next suspension to be used for EPD. The weight-gain amount is shown in Fig. 9 and Table 1. In this case, eight samples were qualified to be analysed with SEM. These samples were coated with following conditions: 3/20, 4/20, 5/20, 2/40, 3/40, 4/40, 5/40 and 2/60. Deposition voltage of 20 V led to the incomplete coating and 60 V led to the formation of microscopic cracks. The SEM images of deposits formed with a voltage of 40 V at different times are presented in Fig. 10. As can be seen in these images, lower durations of 2 and 3 min led to a coating with some pores due to the incomplete deposition. Duration of 3 min was appropriate for formation of a sound coating; however, 5 min led to the crack formation in the coating. The sum of the deposit weights obtained with this suspension was 394.8 mg. The increased number of crack-free coatings compared with 75/25 suspension indicate the positive effect of further ethanol addition on the quality of deposits.

As the next step, the per cent of acetylacetone in the solvent was decreased to 25 vol%. The qualities of deposits formed with these suspensions were better than two mixing ratios of 100 and 75% acetylacetone and were rather similar to 50–50 solvent. In this case, four samples were visually crack free and were analysed with SEM to choose the best ones. These four samples were coated with conditions of 4/20, 5/20, 2/40 and 3 min/40 V.

The weight-gain data for these 16 samples are presented in Table 1 and plotted in Fig. 11. As seen, the sum of the weight gains became even lower to the value of 225.2 mg. This led to the formation of better deposits. The increasing rate of weight

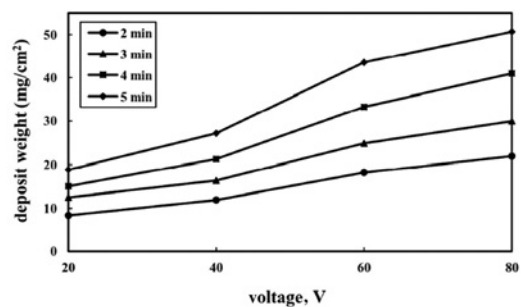


**Fig. 9** Deposited weight versus applied voltage for 50/50 suspension with different durations

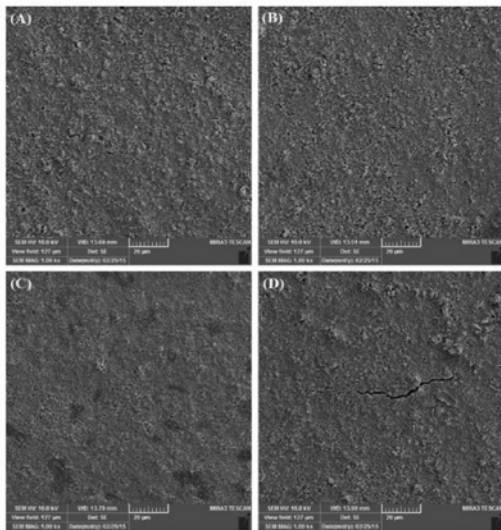


**Fig. 10** SEM images of coatings deposited from 50/50 suspension by voltage of 40 V and durations of  
 a 2 min (CPD = 3%)  
 b 3 min (CPD = 3%)  
 c 4 min (CPD = 2%)  
 d 5 min (CPD = 5%)

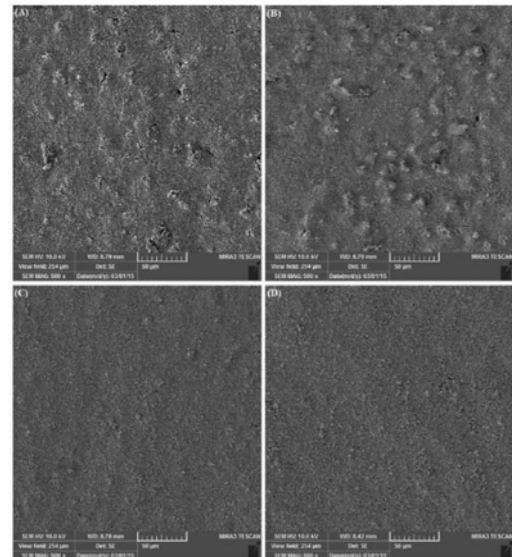


**Fig. 12** SEM images of coatings deposited from 25/75 suspension by conditions of  
 a 4 min/20 V  
 b 5 min/20 V  
 c 2 min/40 V  
 d 3 min/40 V

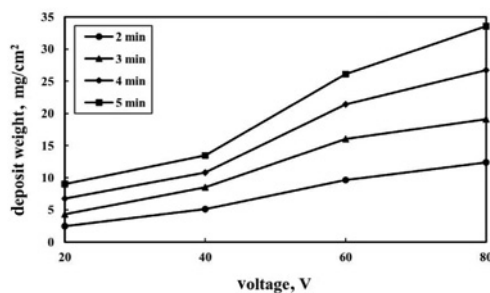


**Fig. 11** Deposited weight versus applied voltage for 25/75 suspension with different durations

gain is obvious in lower voltages and lower durations; however, it shows a decrease in a specified value.

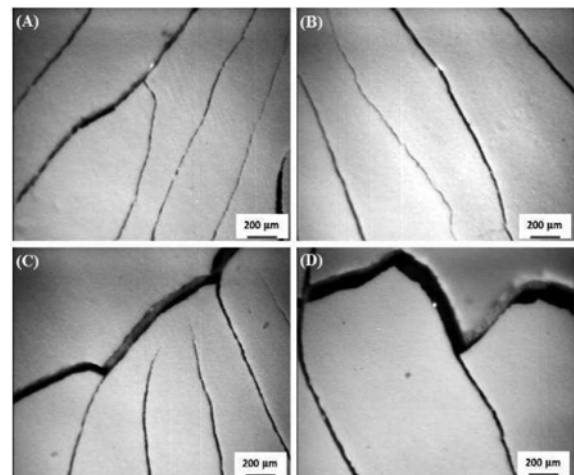
Fig. 12 shows SEM images of the samples with good appearance. As seen in this figure, just two samples with deposition conditions of 2/40 and 3 min/40 V have really crack-free and pore-free structures.

Fig. 13 presents optical microscopic images of deposits formed by a constant voltage of 60 V and durations of 2, 3, 4 and 5 min. This figure not only shows the bad quality of deposits formed by applying 60 V but also presents the role of further process prolonging on the formation of cracks. It should be noted that, though all of the conditions were applied, no EPD occurred from the 0/100 suspension.

It can be inferred from the above results that high applied voltages did not result in sound and crack-free coatings. In case of all suspensions, a descending trend in weight gain was observed when the voltage passed a specific value. This result can be explained by the fact that high applied voltage enhances the average velocity of YSZ particles according to the equation below [12]:

$$v = \mu E \quad (3)$$

in which  $v$  represents the velocity of particles,  $\mu$  is the electrophoretic mobility and  $E$  is the applied electric field. YSZ particles move so fast that the time to arrive at the cathodic substrate is short enough for not arranging particles orderly. This behaviour also can be



**Fig. 13** Optical microscopic images of samples coated from 25/75 suspension with voltage of 60 V and durations of  
 a 2 min (CPD = 10%)  
 b 3 min (CPD = 8%)  
 c 4 min (CPD = 14%)  
 d 5 min (CPD = 18%)

ascribed to the insulation of surface with the formed ceramic layer which leads to the less attraction of charged particles toward the metallic substrate [18, 27].

For comparing the CPDs, it seems some of the resulted cracks are formed due to not well-controlled drying conditions. So, it could be mentioned that by increasing the acetylacetone content (100/0 and 75/25), the evaporation of the remained solvent is slower and the drying cracks should become less than high ethanol containing solvents. However, higher thickness (weight) could compensate the less evaporation rate and increase the cracks (Figs. 5 and 8). In high ethanol containing solvents (25/75), high evaporation rate increases the formation of drying cracks (Fig. 13). Thus, an optimum content of each acetylacetone and ethanol (50/50) could lead to a minimum crack density and an optimum coating thickness (weight) (Fig. 10).

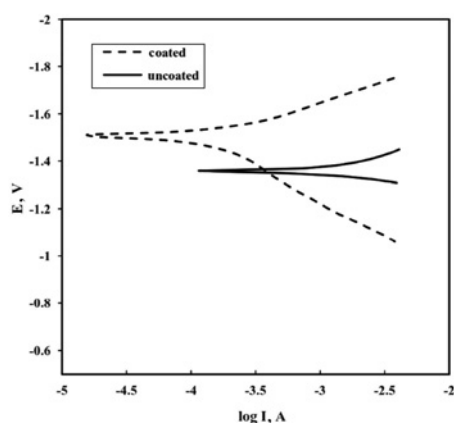


Fig. 14 Potentiodynamic polarisation curves of uncoated and coated magnesium alloys in 3.5% NaCl solution

From above experiments, the deposition conditions were optimised and chosen to be 50/50 suspension, voltage of 40 V and duration of 3 min to obtain a uniform coating. Thereafter, a polarisation experiment was done to observe the protective role of the applied coating. Fig. 14 shows the polarisation curves of coated and naked magnesium alloy. The application of the coating improved the corrosion resistance of the alloy as shown in this figure. The  $I_{\text{corr}}$  and  $E_{\text{corr}}$  values were  $-1.4942$  V and  $0.0883$  mA for coated sample and  $-1.3629$  V and  $1.16$  mA for the uncoated sample.

**4. Conclusions:** In this Letter, three main parameters for EPD, i.e. solid concentration in suspension, deposition voltage and deposition time were studied as well as mixing ratio of solvents in the two-component solvent system in suspension. The following conclusions were drawn according to the observations:

- (i) Zeta potential variations with iodine concentration and solvent type showed that the highest zeta potential and consequently suspension stability is obtained in 50/50 suspension with  $0.5 \text{ g l}^{-1}$  iodine concentration.
- (ii) Mean particle size variations with iodine concentration and solvent type showed that the lowest mean particle size and consequently lowest particle agglomeration is obtained in 50/50 suspension with  $0.5 \text{ g l}^{-1}$  iodine concentration.
- (iii) Acetylacetone and ethanol were used as solvent solely and in a mixed state for EPD of YSZ nanoparticles. It was seen that 100% acetylacetone led to the formation of severe cracks. Besides, 100% ethanol led to taking place of no deposition.
- (iv) The deposit weight increased ascendingly with applied voltage up to a specified voltage but the rate began to fall after that point.

## 5 References

- [1] Zhao M.C., Liu M., Song G., *ET AL.*: 'Influence of the  $\beta$ -phase morphology on the corrosion of the Mg alloy AZ91', *Corros. Sci.*, 2008, **50**, pp. 1939–1953
- [2] 'ASM handbook, vol. 2, properties and selection: nonferrous alloys and special-purpose materials' (ASM International, OH, 1992, 2nd edn.)
- [3] Guo K.W.: 'A review of magnesium/magnesium alloys corrosion and its protection', *Recent Pat. Corros. Sci.*, 2010, **2**, pp. 13–21
- [4] Czerwinski F.: 'Magnesium alloys – corrosion and surface treatments' (INTECH, India, 2011)
- [5] Zhao Q., Guo X., Dang X., *ET AL.*: 'Preparation and properties of composite MAO/ECD coatings on magnesium alloy', *Colloids Surf. B, Biointerfaces*, 2013, **102**, pp. 321–326

- [6] Wang H., Akid R., Gobara M.: 'Scratch-resistant anticorrosion sol-gel coating for the protection of AZ31 magnesium alloy via a low temperature sol-gel route', *Corros. Sci.*, 2010, **52**, pp. 2565–2570
- [7] Hoche H., Blawert C., Broszeit E., *ET AL.*: 'Galvanic corrosion properties of differently PVD-treated magnesium die cast alloy AZ91', *Surf. Coat. Technol.*, 2005, **193**, pp. 223–229
- [8] Christoglou C., Voudouris N., Angelopoulos G.N., *ET AL.*: 'Deposition of aluminium on magnesium by a CVD process', *Surf. Coat. Technol.*, 2004, **184**, pp. 149–155
- [9] Wang Q., Spencer K., Birbilis N., *ET AL.*: 'The influence of ceramic particles on bond strength of cold spray composite coatings on AZ91 alloy substrate', *Surf. Coat. Technol.*, 2010, **205**, pp. 50–56
- [10] Miao Q., Cui C.E., Pan J.D.: 'CrN-TiN multilayer coating on magnesium alloy AZ91 by arc-glow plasma depositing process', *Surf. Coat. Technol.*, 2007, **201**, pp. 5077–5080
- [11] Zhu L., Li W., Shan D.: 'Effects of low temperature thermal treatment on zinc and/or tin plated coatings of AZ91D magnesium alloy', *Surf. Coat. Technol.*, 2006, **201**, pp. 2768–2775
- [12] Besra L., Liu M.: 'A review on fundamentals and applications of electrophoretic deposition (EPD)', *Prog. Mater. Sci.*, 2007, **52**, pp. 1–61
- [13] Corni L., Ryan M.P., Boccaccini A.R.: 'Electrophoretic deposition: from traditional ceramics to nanotechnology', *J. Eur. Ceram. Soc.*, 2008, **28**, pp. 1353–1367
- [14] Stappers L., Zhang L., Van der Biest O., *ET AL.*: 'The effect of electrolyte conductivity on electrophoretic deposition', *J. Colloid Interface Sci.*, 2008, **328**, pp. 436–446
- [15] Ghaleh H.M., Rekabeslami M., Shakeri M.S., *ET AL.*: 'Nano-structured yttria-stabilized zirconia coating by electrophoretic deposition', *Appl. Surf. Sci.*, 2013, **280**, pp. 666–672
- [16] Hornberger H., Virtanen S., Boccaccini A.R.: 'Biomedical coatings on magnesium alloys – a review', *Acta Biomater.*, 2012, **8**, pp. 2442–2455
- [17] Zhu R., Zhang J., Chang C., *ET AL.*: 'Effect of silane and zirconia on the thermal property of cathodic electrophoretic coating on AZ31 magnesium alloy', *J. Magnesium Alloy*, 2013, **1**, pp. 235–241
- [18] Chen F., Liu M.: 'Preparation of yttria-stabilized zirconia (YSZ) films on La<sub>0.85</sub>Sr<sub>0.15</sub>MnO<sub>3</sub> (LSM) and LSM-YSZ substrates using an electrophoretic deposition (EPD) process', *J. Eur. Ceram. Soc.*, 2001, **21**, pp. 127–134
- [19] Hamdy A.S., Farahat M.: 'Chrome-free zirconia-based protective coatings for magnesium alloys', *Surf. Coat. Technol.*, 2010, **204**, pp. 2834–2840
- [20] Das D., Basu R.N.: 'Suspension chemistry and electrophoretic deposition of zirconia electrolyte on conducting and non-conducting substrates', *Mater. Res. Bull.*, 2013, **48**, pp. 3254–3261
- [21] Lee Y.H., Kuo C.W., Shih C.J., *ET AL.*: 'Characterization on the electrophoretic deposition of the 8 mol% yttria-stabilized zirconia nanocrystallites prepared by a sol-gel process', *Mater. Sci. Eng. A*, 2007, **445–446**, pp. 347–354
- [22] Talebi T., Raissi B., Maghsoudipour A.: 'The role of addition of water to non-aqueous suspensions in electrophoretically deposited YSZ films for SOFCs', *Int. J. Hydrog. Energy*, 2010, **35**, pp. 9434–9439
- [23] Aruna S.T., Rajam K.S.: 'A study on the electrophoretic deposition of 8YSZ coating using mixture of acetone and ethanol solvents', *Mater. Chem. Phys.*, 2008, **111**, pp. 131–136
- [24] Bai M., Guo F., Xiao P.: 'Fabrication of thick YSZ thermal barrier coatings using electrophoretic deposition', *Ceram. Int.*, 2014, **40**, pp. 16611–16616
- [25] Xu Z., Rajaram G., Sankar J., *ET AL.*: 'Electrophoretic deposition of YSZ electrolyte coatings for solid oxide fuel cells', *Surf. Coat. Technol.*, 2006, **201**, pp. 4484–4488
- [26] Jia L., Lu Z., Huang X., *ET AL.*: 'Preparation of YSZ film by EPD and its application in SOFCs', *J. Alloys Compd.*, 2006, **424**, pp. 299–303
- [27] Panigrahi S., Besra L., Singh B.P., *ET AL.*: 'Electrophoretic deposition of doped ceria in anti-gravity set-up', *Adv. Powder Technol.*, 2011, **22**, pp. 570–575
- [28] Ahmadi M., Aghajani H.: 'Suspension characterization and electrophoretic deposition of yttria-stabilized zirconia nanoparticles on an iron-nickel based super alloy', *Ceram. Int.*, 2017, **43**, (9), pp. 7321–7328
- [29] Kawakita M., Uchikoshi T., Kawakita J., *ET AL.*: 'Preparation of crystalline-oriented titania photoelectrodes on ITO glasses from a 2-propanol-2,4-pentanedione solvent by electrophoretic deposition in a strong magnetic field', *J. Am. Ceram. Soc.*, 2009, **92**, pp. 984–989
- [30] Sakka Y., Uchikoshi T.: 'Forming and microstructure control of ceramics by electrophoretic deposition (EPD)', *KONA Powder Part. J.*, 2010, **28**, pp. 74–90